NIH RELAIS Document Delivery

NIH-10286727
JEFFDUYN

JOZEF DUYN
10 Center Dirve
Bldg. 10/Rm.1L07
Bethesda, MD 20892-1150

ATTN:		SUBMITTED:	2002-08-29 17:22:18
PHONE:	301-594-7305	PRINTED:	2002-09-05 07:59:48
FAX:	-	REQUEST NO.:	NIH-10286727
E-MAIL:		SENT VIA:	LOAN DOC 7967428

NIH Fiche to Paper Journal

TITLE:	MAGNETIC RESONANCE IN MEDICINE : OFFICIAL JOURNAL OF THE SOCIETY OF MAGNETIC RESONANCE IN MEDICINE / SOCIETY OF MAGNETIC RESONANCE IN MEDICINE
PUBLISHER/PLACE:	Wiley-Liss, Inc., a division of John Wil New York, NY :
VOLUME/ISSUE/PAGES:	1993 Dec;30(6):764-8 764-8
DATE:	1993
AUTHOR OF ARTICLE:	Liu G; Sobering G; Duyn J; Moonen CT
TITLE OF ARTICLE:	A functional MRI technique combining principles of
ISSN:	0740-3194
OTHER NOS/LETTERS:	Library reports holding volume or year 8505245 8139461
SOURCE:	PubMed
CALL NUMBER:	W1 MA34IF
REQUESTER INFO:	JEFFDUYN
DELIVERY:	E-mail: jhd@helix.nih.gov
REPLY:	Mail:

A Functional MRI Technique Combining Principles of Echo-Shifting with a Train of Observations (PRESTO)

Guoying Liu, Geoffrey Sobering, Jeff Duyn, Chrit T. W. Moonen

We present a fast MRI technique sensitized to microscopic susceptibility effects. The method combines elements of echo-shifted gradient-recalled MR imaging (*TE* > *TR*) with the acquisition of multiple *k*-space lines within a single *TR*-period. The sequence results in a much reduced imaging time as compared with conventional gradient-echo MRI methods. The feasibility of the method is demonstrated for susceptibility bolus tracking in the cat brain using an imaging time of 153 ms. The relative cerebral blood volume maps created with this method are comparable with those obtained with conventional methods.

Key words: brain function; rapid MRI; MRI, blood volume; MRI; magnetic susceptibility.

INTRODUCTION

The measurement of changes in microscopic magnetic susceptibility effects forms the basis of two recently developed methods for studying brain activation with MRI. In the first method, the local changes are caused by the transit of a bolus of contrast agent and can be interpreted in terms of relative blood volume (1–5). The second method was designed to measure susceptibility effects, caused by changes in the amount of paramagnetic deoxyhemoglobin (6), and was applied recently in several laboratories (7–14).

In general, changes in microscopic susceptibility effects are measured as changes in T_2* relaxation. Several T_2* sensitized MRI pulse sequences have been used for these types of functional MRI studies, each with distinct advantages and disadvantages. Echo-planar imaging (EPI, 15–17) has high temporal resolution and good signal-to-noise ratio (SNR). However, it requires excellent field homogeneity (18) and hardware that is not generally available on clinical instruments. For measuring T_2* changes, the method suffers from the fact that all *k*-space lines are weighted differently with respect to T_2*. In a typical example, the total encoding period is long compared to the T_2* time constant, even after shimming. In conventional gradient-recalled echo imaging (FLASH, 19–21), all *k*-space lines have identical T_2*-weighting. However, SNR is lower than for EPI. Also, the temporal resolution suffers since the period of T_2*-weighting is shorter than one *TR*-period ($TE < TR$). Recently, we developed the echo-shifted FLASH method (22, 23), where the gradient echo is shifted a variable number of *TR*-periods resulting in $TE > TR$, and thus increasing the temporal resolution.

Here, we combine the Principles of Echo-Shifting with a Train of Observations (PRESTO) for a further reduction of imaging time. This increased imaging speed is caused by the collection of multiple lines of *k*-space in a single *TR*-period. The complete train of gradient echoes is shifted one or more complete *TR*-periods similar to principles previously developed for the echo-shifted gradient-recalled MRI technique (22, 23). The essential feature of the new PRESTO method is the fact that the complete range of T_2*-weighting for all *k*-space lines is small, yet the average weighting remains flexible without changing the total imaging time.

PULSE SEQUENCE

Figure 1a shows the PRESTO pulse sequence. Four gradient-recalled echoes are acquired per *TR*-period and the echo-train is shifted one *TR*-period by the particular slice-selection gradient scheme. Thus, spins excited by the first RF pulse lead to the four gradient echoes during the second *TR*-period. Spins excited by the second RF pulse lead to the four gradient echoes in the third *TR*-period. In general, spins excited in the *n*-th period are refocused four times in the (n + 1)-th *TR*-period. The following gradient characteristics were used:

Slice-Selection Gradient

The slice-selection gradient during the RF pulse is followed by an inverted lobe of equal duration to maintain zero net dephasing for all spins that were excited in the previous *TR*-period. Following the acquisition period, a rephasing gradient pulse is used to rephase spins excited in the current *TR*-period. In order to shift the echo-train **n** *TR*-periods, the amplitude of this rephasing pulse should be divided by n (23).

Read-Out Gradient

A dephasing gradient is followed by a gradient switch scheme such that spins are refocused at the middle of each of the four read-out periods. Furthermore, a rephasing lobe is placed following the echo-train resulting in zero net dephasing within each *TR*-period.

Phase-Encode Gradient

Each gradient echo is phase encoded according to the *k*-space trajectory of Fig. 1b. Thus, the first acquired echo is encoded with the maximum negative phase encoding.

MRM 30:764–768 (1993)

From the *in Vivo* NMR Research Center, BEIP, NCRR (G.L., G.S., J.D., C.T.W.M.); and the Laboratory for Diagnostic Radiology Research (J.D.), National Institutes of Health, Building 10, Room B1D-123, Bethesda, Maryland.

Address correspondence to: Chrit T. W. Moonen, in Vivo NMR Research Center, BEIP, NCRR, National Institutes of Health, Building 10, Room B1D-123, Bethesda, MD 20892.

Received May 7, 1993; revised July 29, 1993; accepted August 11, 1993.

0740-3194/93 $3.00

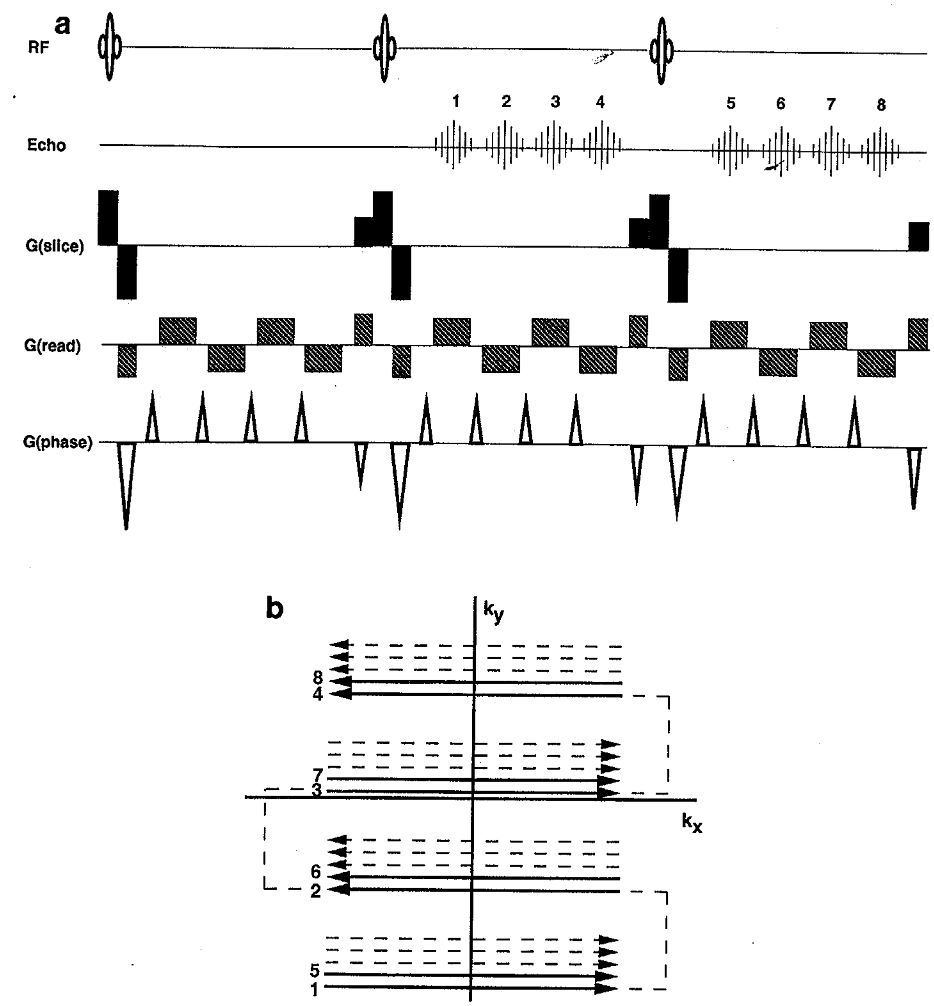

FIG. 1. (a) Pulse sequence for the PRESTO method. The echo-train is shifted by one *TR*-period by the particular slice-selection gradient arrangement. The echo-train is generated by the read-out gradient switch scheme leading to the acquisition of four *k*-space lines per *TR*-period. The phase encoding consists per *TR*-period of a large negative lobe, four constant "blips" and a rewinder. The dephasing lobe and rewinder are incremented for each *TR*-period. (b) The *k*-space sampling trajectory for the PRESTO pulse sequence of Fig. 1a. The consecutive numbering of echoes in Fig. 1a corresponds with their *k*-space location as shown on the left. Thus, the first acquired echo is encoded with the maximum negative phase encoding. The phase-encoding "blip" between subsequent echoes increases the phase by one quarter of the full k_y-space (indicated by the dashed line) leading to four *k*-space lines per *TR*-period. In the next *TR*-period, the entire sequence is repeated with the negative dephasing lobe incremented according to the field-of-view. Thus, *k*-space is divided in four blocks, with the first block sampled by the first echo of all *TR*-periods, the second block by the second echo of all *TR*-periods, etc.

The "blip" between subsequent echoes increases the phase corresponding to one quarter of the full k_y-space. The use of four 'blips' instead of three is to maintain a better symmetry in the pulse sequence and thus to minimize the effects of residual gradients. Phase-encoding rewinders are used at the end of each *TR*-period to bring spins back in phase prior to the next RF excitation as described elsewhere (23, 24). In the next *TR*-period, the initial dephasing lobe and the rewinder lobe are incremented, whereas the "blips" remain identical. Note that this trajectory is similar to that used for the GRASE technique and results in reduced phase encode artifacts (25).

Several fine adjustments in gradient amplitudes (tweakers) were implemented in the pulse sequence: a) phase-encoding 'blip' adjustment, b) dead time adjustment placed between onset of read gradient and echo sampling, c) tweaking of the slice-selection gradient rephasing lobe. The first serves to adjust each 'blip' to a phase increment corresponding to exactly one quarter of k_y-space. The second tweaker serves to eliminate a timing mismatch between the periods of echo sampling and read-out gradient. Residual gradients or small gradient mismatch may also necessitate this tweaker. The third serves to rephase all spins in the slice. On our instrument, the first tweaker was insignificant. However, the dead time adjustment was necessary in order to align the echoes scanned in opposite k_x directions (i.e., the four blocks in *k*-space, see Fig. 1b). The third tweaker is generally small, but optimizes the SNR for the slice. The use of four phase encode "blips" instead of three also proved not to be necessary for good image quality.

For a 64 × 64 image, 17 *TR*-periods are needed since no signal is collected in the first *TR*-period. When a dynamic experiment is performed with continuous imaging, 16 *TR*-periods suffice since signal excitation for the echoes acquired during the first *TR*-period can be performed by the last RF pulse of the previous image.

After acquisition, the echoes collected with negative read-out gradients were reversed, and all the echoes were reshuffled into their proper positions in *k*-space. A standard 2DFT reconstruction was then used to generate the image.

MATERIAL AND METHODS

The experiments were performed on a GE 4.7 T Omega CSI instrument equipped with shielded gradients having a maximum strength of 0.18 T/m. A home-made 4.7-cm diameter surface coil was used for the cat study. The animals were ventilated using isoflurane (1%) and a N_2O/O_2 mixture (7:3); blood pressure, blood gases, and

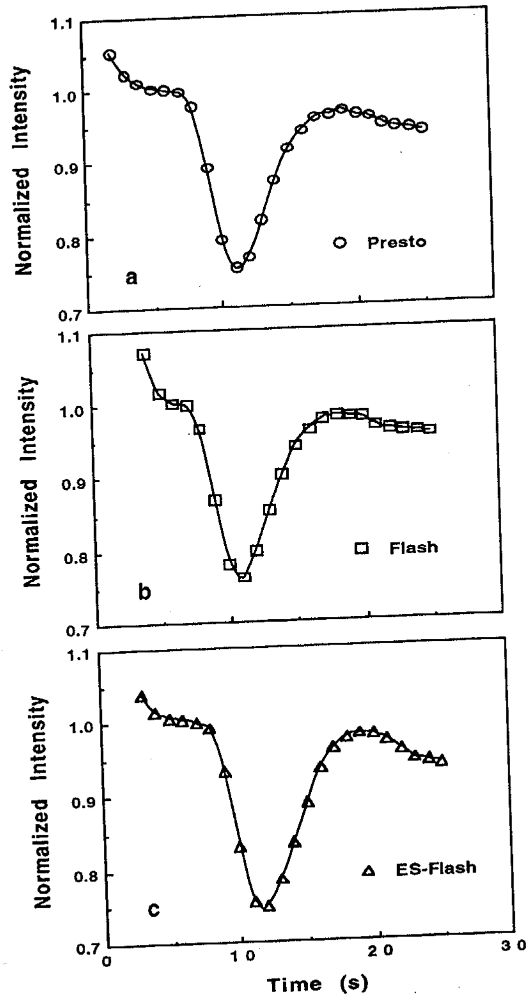

FIG. 2. Time dependence of the normalized intensity (with respect to pre-bolus steady state) obtained from an axial slice of a cat brain as a function of time for (a) the PRESTO sequence (*TE* 13.5 ms, *TR* 9.0 ms, time per image 153 ms); (b) the conventional FLASH sequence (*TE* 13.5 ms, *TR* 16.0 ms, time per image 1 s); and (c) the ES-FLASH sequence (*TE* 13.5 ms, *TR* 9.0 ms, time per image 576 ms). The bolus of Gd-DTPA was injected shortly after the pulse sequence started. A 10° RF flip angle was used. The region of interest consisted of all voxels within the brain boundaries.

heart rate were monitored and kept normal. Succinylcholine (0.8%) was used as a muscle relaxant. For blood-volume measurements, 0.03 mmol/kg Gd-DTPA (Magnevist, BERLEX) was injected as a bolus in the femoral vein shortly after continuous imaging started.

Shimming was performed on the slice of interest resulting in a line width of about 18 Hz at half height of the water resonance. Slice selection was performed using a three-lobed sinc RF pulse with a duration of 500 µs and a flip angle of about 10°. The slice thickness was 5 mm and the field of view was 64 mm giving a nominal in-plane resolution of 1 mm for the 64 × 64 axial images. The field strength for the slice-selection gradient during the RF pulse was 56 mT/m and the ramp time for the gradient pulse was 275 µs. The dephasing of the slice-selection gradient combination leads to a signal attenuation of more than 95% for the unwanted primary echoes as calculated previously (23). Due to the small flip angle the contribution of spin echoes and stimulated echoes is even further attenuated. Each of the read-out gradient periods was 800 µs corresponding exactly to the echo sampling interval. The ramp time was 550 µs to switch the polarities of the read-out gradient. The effective echo time (*TE*), the time interval between spin excitation and the center of the gradient echo-train formed in the subsequent *TR*-period, was 13.5 ms. The length of the train of four echoes in each *TR*-period was 4.8 ms measured from the start of the first echo until the end of the fourth echo. The repetition time (*TR*), the interval between RF pulses, was 9.0 ms leading to a total imaging time of 153 ms for a 64 × 64 matrix. For comparison, a conventional FLASH method was used with a *TR* of 16.0 ms (*TE* 13.5 ms) leading to an imaging time of 1 s. The results were also compared with an ES-FLASH method (*TR* 9.0 ms, *TE* 13.5 ms) with an imaging time of 576 ms. Due to data storage limitations in our instrument hardware it was not possible to continuously image during the complete first passage of the bolus with the PRESTO technique. Thus, for this comparative study, 847 ms, 424 ms, and zero time delays were used between successive images for PRESTO, ES-FLASH, and FLASH methods, respectively, thus resulting in an actual time resolution of 1 s per image for each method. The delay between acquisition of successive images resulted in slightly different steady-state magnetization for PRESTO, ES-FLASH, and FLASH. RF pulse angles were always lower than the Ernst flip angle in order to limit these effects. However, the remaining differences in steady-state magnetization complicate a direct signal to noise comparison between the methods. All other parameters of the three methods were identical except the read-out gradient strength (29 mT/m for PRESTO, 7 mT/m for both FLASH and ES-FLASH), resulting from a read-out period four times shorter for each echo in PRESTO.

RESULTS AND DISCUSSION

The PRESTO experiment was tested on a spherical phantom containing pure water. The echo-shifting principles were first tested by switching off all phase-encoding gradients and comparing the primary (unwanted) gradient echo amplitude with that of the shifted echoes. The primary echoes were attenuated more than 95% as compared to the amplitude of the shifted echoes. The actual T_2* sensitivity in the PRESTO technique was compared to that in a FLASH method with long *TR*. The effective *TE* for PRESTO is the time interval between signal excitation and the center of the shifted echo-train. T_2* values of 208 and 206 ms were measured for the phantom using PRESTO and FLASH, respectively, confirming the similar signal decay upon increasing *TE* corresponding to local field homogeneity. A comparison of SNR between PRESTO and FLASH was carried out on phantoms. As predicted from the four times higher bandwidth for PRESTO in these measurements, the SNR for PRESTO is half that of the FLASH method.

The PRESTO sequence was used to assess relative cerebral blood volume (rCBV) in the cat brain by the method of dynamic contrast-enhanced susceptibility imaging according to principles published recently (1–3). Figure 2 shows the time course of the signal intensity changes in the cat brain following the injection of a bolus of Gd(DTPA) using PRESTO and, for comparison, FLASH, and ES-FLASH. At the top of the bolus, a signal decrease of 25%, 24%, and 26% was determined for PRESTO, FLASH, and ES-FLASH, respectively. The similar intensity-time curves confirm that PRESTO has the same sensitivity to dynamic susceptibility changes as the other two methods.

Figure 3 displays single-slice 64 × 64 images of cat brain immediately before bolus injection (pre-bolus) and at the highest concentration of contrast agent (bolus maximum). As can be seen, relatively high quality images can be recorded using PRESTO without apparent ghosting artifacts. The dynamic susceptibility effect caused by the contrast agent is demonstrated similarly with the new method, yet at a much higher imaging speed.

Changes in brain signal intensity due to transit of the bolus can be converted to contrast agent concentration-time curves for each voxel as explained previously (1–5). The area under the concentration-time curve is proportional to blood volume according to conventional tracer kinetics theory (26, 27). The relative cerebral blood volume maps generated in this way are comparable for all three methods (Fig. 3). The blood volume maps show an expected contrast between white and gray matter. A conventional spin-echo image is given in Fig. 4 to outline the anatomical features of the slice.

Note that the signal loss in areas of high macroscopic susceptibility in the frontal areas (superior to the eyes) is apparent in all three methods. These features are absent in the calculated blood volume maps and their macroscopic features correspond closely to the white-grey matter outline as shown by the spin-echo image.

We conclude that the PRESTO technique is a very fast, T_2* sensitized, MRI method. The disadvantage is that the SNR is not as high as that of EPI because of the decreased steady-state magnetization. Its main advantage is that the full *k*-space is acquired within a narrow range of T_2*-weighting. The average T_2*-weighting can be altered by shifting the echo-train a variable number of *TR*-periods. These features also result in substantially lower field

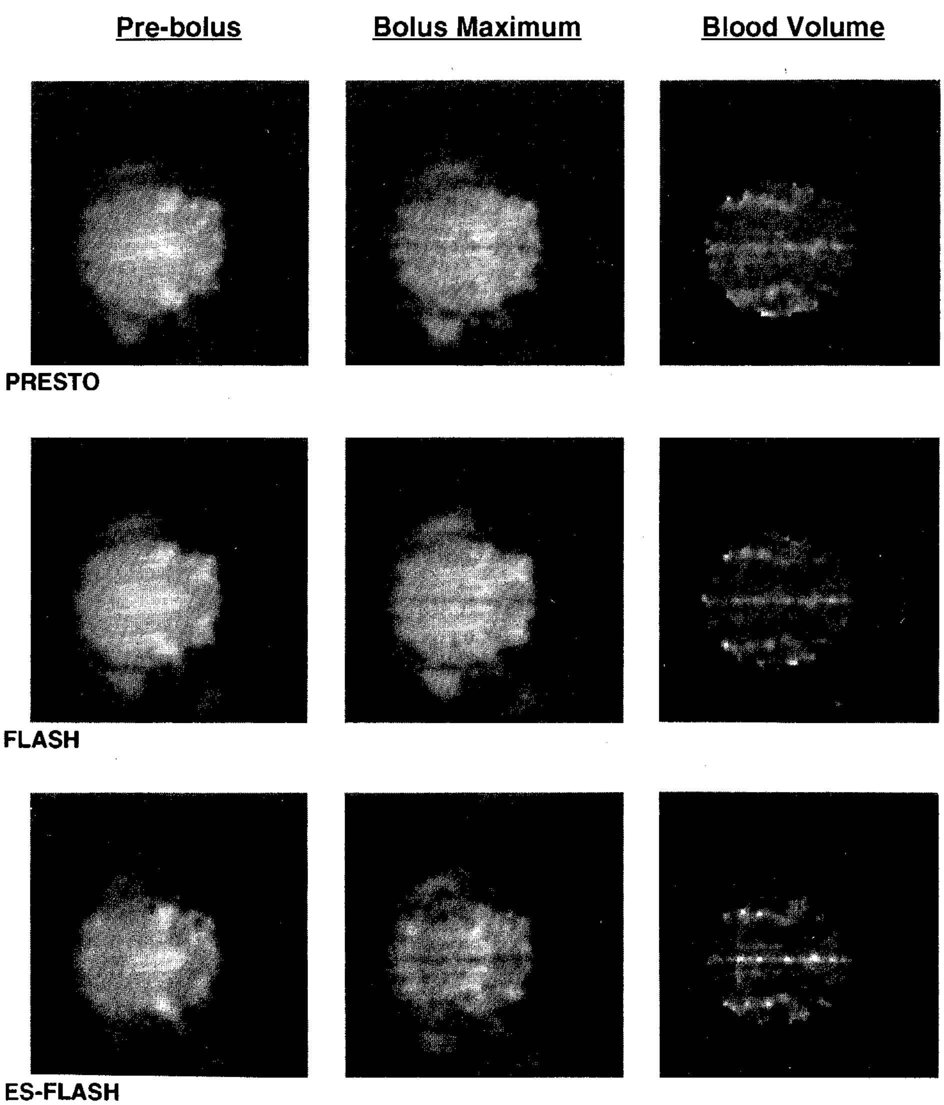

FIG. 3. Axial slice images (64 × 64 mm field-of-view, 64 × 64 data matrix) of the cat brain obtained before injection of the bolus (column 1), at the maximum concentration of the bolus (column 2), and calculated rCBV map (column 3) using the PRESTO method (row 1, *TE* 13.5 ms, *TR* 9.0 ms, time per image 153 ms), the FLASH method (row 2, *TE* 13.5 ms, *TR* 16.0 ms, time per image 1 s), and the ES-FLASH method (row 3, *TE* 13.5 ms, *TR* 9.0 ms, time per image 576 ms). A circular cosine-bell filter with a flat profile over the central 90% of the *k*-space central axes was applied to the raw data after reshuffling.

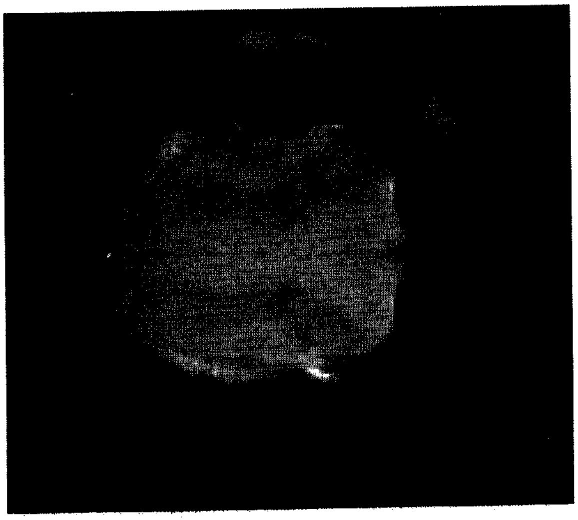

FIG. 4. Image obtained with the conventional spin-echo method (128 × 128 data matrix) with TE 60 ms, TR 1 s through the same axial slice of the cat brain (64 × 64 mm field-of-view).

homogeneity requirements than EPI. In addition, the sequence does not impose stringent demands on hardware, and the size of the data matrix is flexible because of the segmentation of k-space.

REFERENCES

1. A. Villringer, B. R. Rosen, J. W. Belliveau, J. L. Ackerman, R. B. Lauffer, R. B. Buxton, Y. S. Chao, V. J. Wedeen, T. J. Brady, *Magn. Reson. Med.* **6,** 164 (1988).
2. J. W. Belliveau, D. N. Kennedy, R. C. McKinstry, B. R. Buchbinder, R. M. Weisskoff, M. S. Cohen, J. M. Vivea, T. J. Brady, B. R. Rosen, *Science* **254,** 716 (1990).
3. B. R. Rosen, J. W. Belliveau, D. Chien, *Magn. Reson. Q.* **5,** 263 (1989).
4. J. R. Zigun, J. A. Frank, F. A. Barrios, D. W. Jones, T. K. F. Foo, C. T. W. Moonen, D. Z. Press, D. R. Weinberger, *Radiology* **186,** 353 (1993).
5. C. T. W. Moonen, P. C. M. van Zijl, D. Le Bihan, J. Frank, E. D. Becker, *Science* **250,** 53 (1990).
6. S. Ogawa, T. M. Lee, A. R. Kay, D. W. Tank, *Proc. Natl. Acad. Sci. (USA)* **87,** 9868 (1990).
7. R. Turner, D. Le Bihan, C. T. W. Moonen, D. DesPres, J. Frank, *Magn. Reson. Med.* **22,** 159 (1991).
8. P. A. Bandettini, E. C. Wong, R. S. Hinks, R. S. Tikofsky, J. S. Hyde, *Magn. Reson. Med.* **25,** 390 (1992).
9. K. K. Kwong, J. W. Belliveau, D. A. Chesler, I. E. Goldberg, R. M. Weisskoff, B. P. Poncelet, D. N. Kennedy, B. E. Hoppel, M. S. Cohen, R. Turner, H. M. Cheng, T. J. Brady, B. R. Rosen, *Proc. Natl. Acad. Sci. (USA)* **89,** 5675 (1992).
10. S. Ogawa, D. W. Tank, R. Menon, J. M. Ellermann, S. G. Kim, H. Merkle, K. Ugurbil, *Proc. Natl. Acad. Sci. (USA)* **89,** 5951 (1992).
11. J. Frahm, H. Bruhn, K. D. Merboldt, W. Hänicke, *J. Magn. Reson. Imaging* **2,** 501 (1992).
12. J. Frahm, K. D. Merboldt, W. Hänicke, *Magn. Reson. Med.* **29,** 139 (1993).
13. R. Turner, P. Jezzard, H. Wen, K. K. Kwong, D. Le Bihan, T. Zeffiro, R. S. Balaban, *Magn. Reson. Med.* **29,** 277 (1993).
14. A. M. Blamire, G. MacCarthy, R. Gruetter, D. L. Rothman, Z. Rattner, F. Hyder, R. G. Shulman, *in* "Book of Abstracts, 11th Annual Meeting, Society of Magnetic Resonance in Medicine, Berlin, 1992," p. 1834.
15. P. Mansfield, *J. Phys.* **C10,** L55 (1977).
16. P. Mansfield, I. L. Pykett, *J. Magn. Reson.* **29,** 355 (1978).
17. P. Mansfield, A. A. Maudsley, *J. Magn. Reson.* **27,** 101 (1977).
18. F. Farzaneh, S. J. Riederer, N. J. Pelc, *Magn. Reson. Med.* **14,** 123 (1990).
19. A. Haase, J. Frahm, D. Matthaei, W. Hänicke, K. D. Merboldt, *J. Magn. Reson.* **67,** 258 (1986).
20. A. Haase, D. Matthaei, W. Hänicke, J. Frahm, *Radiology* **160,** 537 (1986).
21. F. W. Wehrli, *Magn. Reson. Q.* **6,** 165 (1990).
22. C. T. W. Moonen, G. Liu, P. van Gelderen, G. Sobering, *Magn. Reson. Med.* **26,** 184 (1992).
23. G. Liu, G. Sobering, A. W. Olson, P. van Gelderen, C. T. W. Moonen, *Magn. Reson. Med.* **30,** 68 (1993).
24. J. Frahm, K. D. Merboldt, W. Hänicke, *J. Magn. Reson.* **27,** 307 (1987).
25. K. Oshio, D. A. Feinberg, *Magn. Reson. Med.* **20,** 344 (1991).
26. S. S. Kety, C. F. Schmidt, *J. Clin. Invest.* **27,** 476 (1948).
27. N. A. Lassen, W. Perl, *in* "Tracer Kinetic Methods in Medical Physiology," Raven Press, New York, 1979.